The $[Me_2AlOAlMe_2]\cdot PhOMe$ complex was obtained from equimolar reaction of $[Me_2AlOLi]\cdot PhOMe$[14] and Me_2AlCl in hexane; mp −16°; yield, *ca.* 50% after recrystallization from *n*-hexane at −50°. For nmr data, see Table IV. Upon distillation, the $[AlMe_3]\cdot PhOMe$ complex was eluted, leaving a polymeric material of $-(MeAlO)_n-$. The $[AlMe_3]\cdot PhOMe$ complex was colorless needles at −78° and was nmr spectroscopically identical with the complex prepared from $AlMe_3$ and anisole (see Table IV).

$[Et_2AlOAlEt_2]\cdot StO$. In the presence of $Et_2AlOAlEt_2$ an equimolar amount of styrene oxide (StO) was added dropwise at −20°. Colorless needles were formed instantaneously in a yield of *ca.* 60%; mp −10 to −20°. The complex was soluble in benzene. Similary, **$[Me_2AlOAlMe_2]\cdot StO$** could be obtained as needlelike crystals melting at *ca.* −20° in *ca.* 70% yield. Hydrolysis of these compounds gave the corresponding alkanes and styrene oxide polymers.

Triethylbornyldialuminoxane, $Et_2AlOAlEt(OC_{10}H_{17})$. Equimolar reaction of Et_2AlCl and borneol at −20° in toluene afforded $EtClAl(OC_{10}H_{17})$ as needlelike crystals. *Anal.* Calcd for $C_{12}H_{22}OClAl$: Al, 11.0. Found: Al, 9.5. This bornylate was allowed to react with Et_2AlOLi in hexane to give crystalline products when concentrated under reduced pressure. It was recrystallized from *n*-hexane; yield, *ca.* 60% after recrystallization. Hydrolysis of the compound resulted in 95% of the theoretical amount of ethane and in 98% of that of borneol.

Triethylacetylacetonatodialuminoxane, $Et_2AlOAlEt(acac)$. Equimolar reaction of EtAlCl(acac) (colorless liquid, bp 58° (0.5 mm), containing 13.7% Al (calcd, 14.2)) with Et_2AlOLi gave an oily compound in a yield of *ca.* 85%. Prisms grown from the compound upon storage were confirmed as $Al(acac)_3$ by comparing with the authentic sample; yield, *ca.* 30%.

Analyses. The Al content was determined volumetrically by the 8-hydroxyquinoline method. Analysis of Li was performed according to the method described by Ziegler[31] for the analysis of $LiAlH_4$. The neutralization point in the titration was found to be at around pH 7 independent of the ratio of Li to Al. Gasometry was undertaken according to the method described previously.[14] Molecular weights of the organoaluminum compounds were measured cryoscopically in the benzene solutions.

(31) K. Ziegler and H. G. Gellert, *Justus Liebigs Ann. Chem.*, **589**, 7 (1954).

Spectroscopy. A Nihon Bunko Type DS-402G infrared spectrometer was employed for the ir spectroscopy of the organoaluminum compounds in cyclohexane solution. A variable-spacing cell device was used for the compensation techniques. Nmr spectra of the benzene or benzene-d_6 solutions of the organoaluminum compounds were recorded with a Varian A-60 spectrometer (60 MHz) at room temperature. The chemical shifts were externally standardized with TMS (δ 0.00) or internally standardized with the benzene protons (δ 6.57, an average value of the benzene protons in the presence of the organoaluminum compounds when externally standardized with TMS).

Electric Conductivity. The specific conductivities of the organoaluminum compounds, sealed under argon, were determined in toluene (10^{-1}–10^{-3} *M*) at 25° using an alternating current potentiometer for the samples of higher conductivity and a direct current galvanometer for those of lower conductivity. The latter can detect 10^{-12} A. The cells (cell constant $K = 0.41470$ and 0.44638) contain 10 mm × 10 mm platinum black electrodes.

Acknowledgments. The authors express their thanks to Dr. T. Aoyagi and Mr. Y. Nakano for instrumentations of the conductometric apparatus and also to Mr. S. Ishikawa for recording of the ir spectra.

Registry No. Et_2AlOLi, 20888-82-8; $(i\text{-}Bu)_2AlOLi$, 31471-19-9; $(i\text{-}Bu)_2AlONa$, 41156-38-1; Me_2AlOLi, 31390-21-3; $Et_2AlOAlEt_2$, 1069-83-6; Et_2AlCl, 96-10-6; $(i\text{-}Bu)_2AlOAl(i\text{-}Bu)_2$, 998-00-5; $(i\text{-}Bu)_2AlCl$, 1779-25-5; $Me_2AlOAlMe_2$, 29429-58-1; $Et_2AlOAlMe_2$, 41021-32-3; EtMeAlOAlEtMe, 29429-59-2; $[Et_2AlOAlEt_2]\cdot BQ$, 40961-82-8; $[Et_2AlCl]\cdot BQ$, 41021-42-5; $[Me_2AlCl]\cdot BQ$, 40961-83-9; $[Me_2AlOAlMe_2]\cdot BQ$, 40961-84-0; $[Et_2AlOAlMe_2]\cdot BQ$, 39322-86-6; $[Et_2AlOAlEt_2]\cdot BQ_2$, 40961-85-1; $[Et_2AlOLi]\cdot BQ$, 40902-30-5; $[Et_2AlOAlEt_2]\cdot THF$, 40961-87-3; $[Et_2AlCl]\cdot THF$, 40961-88-4; $[Me_2AlOAlMe_2]\cdot THF$, 40961-89-5; $[Me_2AlCl]\cdot THF$, 41007-93-6; $[Me_2AlOAlMe_2]\cdot PhOMe$, 40961-90-8; $[AlMe_3]\cdot PhOMe$, 20791-22-4; $[Et_2AlOAlEt_2]\cdot StO$, 40961-92-0; $[MeAlOAlMe_2]\cdot StO$, 40961-86-2; $Et_2AlOAlEt(OC_{10}H_{17})$, 40907-47-9; $EtClAl(OC_{10}H_{17})$, 41021-33-4; $Et_2AlOAlEt(acac)$, 24803-77-8; Me_2AlCl, 1184-58-3; $[Me_2AlOLi]\cdot PhOMe$, 40902-31-6; $C_{10}H_{17}OH$, 507-70-0; EtAlCl(acac), 40961-78-2; $[Et_3Al]\cdot BQ$, 40961-79-3; $[Me_3Al]\cdot BQ$, 40961-80-6.

Contribution from the Department of Chemistry, University of Massachusetts, Amherst, Massachusetts 01002

Pentacoordinated Molecules. XVIII.[1] Molecular Structure of Bis(*tert*-butyl)trifluorophosphorane from Infrared and Laser Raman Spectroscopy

ROBERT R. HOLMES,* G. TING-KUO FEY,[2a] and ROBERT H. LARKIN[2b]

Received October 3, 1972

The liquid-state infrared spectrum of bis(*tert*-butyl)trifluorophosphorane was recorded in the range 3000–33 cm^{-1}. Corresponding Raman displacements are reported as well as polarization measurements. Detailed assignments of the fundamental frequencies are shown to be consistent with C_s symmetry with strong preference given to a trigonal bipyramid with equatorially oriented *tert*-butyl groups. The C_s symmetry suggests a staggered conformation for the neighboring *tert*-butyl groups and the presence of hindered rotation due to the mutual steric interference of these groups. Comparison of fundamental frequencies with those of related *tert*-butylphosphorus compounds and trifluorophosphoranes reveals a correlation between increasing axial PF stretching frequency and increasing group electronegativity in the series X_2PF_3 as X is changed.

Introduction

Vibrational analysis has established the structural symmetry of several members of the pentacoordinate series X_2PF_3 (where X = Cl,[3] Br,[4] H,[1,5,6] and CH_3[7]). In each instance, a trigonal-bipyramidal framework with the X lig-

(1) Presented in preliminary form at the 163rd National Meeting of the American Chemical Society, Inorganic Division, Boston, Mass., April 9–14, 1972, paper 47. Previous paper: R. R. Holmes and C. J. Hora, *Inorg. Chem.*, 11, 2506 (1972).

(2) (a) Taken in part from the thesis submitted by G. T. Fey to the Department of Chemistry in partial fulfillment of the Ph.D. degree; (b) Department of Chemistry, Massachusetts Institute of Technology, Cambridge, Mass., 02139.

(3) J. E. Griffiths, R. P. Carter, Jr., and R. R. Holmes, *J. Chem. Phys.*, 41, 863 (1964).

(4) J. A. Salthouse and T. C. Waddington, *Spectrochim. Acta, Part A*, 23, 1069 (1967).

(5) R. R. Holmes and R. N. Storey, *Inorg. Chem.*, 5, 2146 (1966).

(6) J. Goubeau, R. Baumgartner, and H. Weiss, *Z. Anorg. Chem.*, 348, 286 (1966).

(7) A. J. Downs and R. Schmutzler, *Spectrochim. Acta, Part A*, 23, 681 (1967).

ands occupying equatorial positions is strongly supported and agrees with corresponding ^{19}F nmr data on these substances.[8-10] In addition, detailed structural parameters are available from an electron diffraction study[11] for the $(CH_3)_2PF_3$ member.

It is of interest to extend the range of substituent electronegativity in this series as well as to consider the neighboring effect of bulky groups. Consequently, the vibrational analysis of bis(*tert*-butyl)trifluorophosphorane was undertaken in this study.

Previously, we had carried out a similar study[12] on *tert*-butyltetrafluorophosphorane. Here, as in other members of the series XPF_4,[13] the expected trigonal-bipyramidal structure resulted with the *tert*-butyl group present in an equatorial site. It might be anticipated that mutual steric repulsion of the two *tert*-butyl groups in X_2PF_3 would favor a D_{3h} conformation with axially oriented *tert*-butyl ligands. Our study, however, shows this not to be the case. The low molecular symmetry obtained (C_s) supports equatorially positioned *tert*-butyl groups arranged in a staggered conformation.

Important, too, is the understanding of the transmission of electronic effects as the ligand electronegativity is reduced. As ^{19}F nmr has indicated,[8,9,14] the trend[15] in the series X_2PF_3 (where X = Cl, CH_3, and *tert*-butyl) is an upfield shift, in agreement with electronegativity considerations, in contrast to the downfield shift observed[8,16] along the Cl_nPF_{5-n} series. In the case of the *tert*-butyl series (*tert*-butyl)PF_{5-n} where $n = 1$-3, the trend[15] in chemical shifts[14] is slightly upfield as n increases.

Additional data bearing on electronic effects supplied by vibrational analyses[7] have shown that, in the series $(CH_3)_n$-PF_{5-n} (where $n = 0$-3), the change in axial stretching frequency and associated force constant parallels the change in axial bond distance.[11,17] The decreased stability indicated with increased methyl substitution agrees with the Gillespie[18] electron-pair repulsion scheme. Extension of the vibrational analysis to include the bis(*tert*-butyl) derivative might allow a similar correlation in the *tert*-butyl series and prove helpful in estimating the relative importance of electronic *vs.* steric effects in pentacoordinate phosphorus compounds.

Experimental Section

The usual precautions in handling air-sensitive compounds were taken using inert atmosphere glove bag techniques for transfer operations and Schlenk type glassware in the preparations. Halocarbon grease was used on all ground joints.

Bis(*tert*-butyl)trifluorophosphorane was prepared following the method of Fild and Schmutzler.[14] This consisted of fluorinating bis(*tert*-butyl)chlorophosphine[19] $[(CH_3)_3C]_2PCl$ with excess SbF_3 at 100°. The product was obtained as a colorless liquid. It was purified by distillation under reduced pressure, bp 76–77° (52 mm) [lit.[14] 76° (52 mm)]. *Anal.* Calcd for $C_8H_{18}PF_3$: C, 47.52; H, 8.97; P, 15.32; F, 28.19. Found: C, 47.50; H, 9.00; P, 15.30; F, 28.18.

A Beckman IR 11-12 spectrophotometer was used to record the infrared spectrum of $[(CH_3)_3C]_2PF_3$ in the 3000–400-cm^{-1} region on the pure liquid film employing cells with KBr windows. The far-infrared spectrum (650–33 cm^{-1}) was also studied with the same instrument using polyethylene cells of varying path lengths (Barnes Eng. Co.). The instrument in both cases was flushed with dry nitrogen and calibrated as before.[12]

The Raman spectrum of the liquid was recorded on a Cary 82 spectrophotometer employing a CRL Model 52B argon ion laser. Displacements from the 5145-Å line were obtained. The liquid samples were present in 5-mm Pyrex tubes sealed directly from the vacuum distillation process. Polarization measurements were carried out with the use of a polarization analyzer orienting the electric vector of the laser excitation light perpendicular and parallel to the electric vector of the Raman radiation. In addition, the Raman spectrum of the solid phase was recorded with the aid of a low-temperature cell of the Harney–Miller type.[20]

Results

The liquid-state infrared spectrum for $[(CH_3)_3C]_2PF_3$ from 3000 to 400 cm^{-1} is shown in the upper part of Figure 1, the Raman spectrum in the middle, and the far-infrared spectrum in the lower part. Polarized Raman spectra are displayed in Figure 2. Table I lists the frequencies, relative intensities, states of polarization, and suggested assignments.

The interpretation of the vibrational spectrum for a molecule as complex as $[(CH_3)_3C]_2PF_3$ is aided to a large extent by considering the assignment of the *tert*-butyl groups independent from that of the skeletal vibrations of the C_2PF_3 unit. It is found that the portion of the spectrum assigned to the *tert*-butyl grouping changes little from that of related compounds such as $[(CH_3)_3C]_2PF$,[21] $[(CH_3)_3C]_2PCl$,[21] and the corresponding monosubstituted derivatives.[22,23] Additional simplification is obtained by treating the fundamental vibrations of the *tert*-butyl group in terms of C_{3v} local symmetry. Even though the molecular symmetry proves lower, no alteration in selection rules from symmetric top molecules is apparent.

Lastly, coupling between the two *tert*-butyl groups is not evident, at least, under the spectral resolution reported here. The only obvious splittings of in-phase and out-of-phase modes arise from the symmetric and antisymmetric PC stretches. The skeletal modes for the C_2PF_3 framework are assigned on the basis of C_s symmetry, the justification for which is presented below.

Possible structural models are shown in Figure 3: three trigonal bipyramids and three tetragonal pyramids of various symmetries. Both a low and high barrier case with respect to rotation of the *tert*-butyl groups about the PC bonds are considered for each structure. Table II lists the corresponding selection rules for the point group symmetries associated with the structures in Figure 3.

Structures III, IV, and V are ruled out as sterically unfavorable in that they position the two *tert*-butyl groups at C-P-C angles near 90°. Taking advantage of the charac-

(8) R. R. Holmes, R. P. Carter, Jr., and G. E. Peterson, *Inorg. Chem.*, 3, 1748 (1964).
(9) (a) E. L. Muetterties, W. Mahler, and R. Schmutzler, *Inorg. Chem.*, 2, 613 (1963); (b) E. L. Muetterties, W. Mahler, K. J. Packer, and R. Schmutzler, *ibid.*, 3, 1298 (1964).
(10) P. M. Treichel, R. A. Goodrich, and S. B. Pierce, *J. Amer. Chem. Soc.*, 89, 2017 (1967).
(11) L. S. Bartell and K. W. Hansen, *Inorg. Chem.*, 4, 1777 (1965).
(12) R. R. Holmes and M. Fild, *Inorg. Chem.*, 10, 1109 (1971).
(13) R. R. Holmes and M. Fild, *J. Chem. Phys.*, 53, 4161 (1970), and references cited therein.
(14) M. Fild and R. Schmutzler, *J. Chem. Soc. A*, 2359 (1970).
(15) R. R. Holmes, *Accounts Chem. Res.*, 5, 296 (1972).
(16) (a) R. R. Holmes and W. P. Gallagher, *Inorg. Chem.*, 2, 433 (1963); (b) R. P. Carter, Jr., and R. R. Holmes, *ibid.*, 4, 738 (1965).
(17) K. W. Hansen and L. S. Bartell, *Inorg. Chem.*, 4, 1775 (1965).
(18) (a) R. J. Gillespie and R. S. Nyholm, *Quart. Rev., Chem. Soc.*, 11, 339 (1957); (b) R. J. Gillespie, *Can. J. Chem.*, 38, 818 (1960); (c) R. J. Gillespie, *J. Chem. Educ.*, 40, 295 (1963).
(19) (a) W. Voskuil and J. F. Arens, *Recl. Trav. Chim. Pays-Bas*, 82, 302 (1963); (b) M. Fild, O. Stelzer, and R. Schmutzler, private communication.
(20) F. A. Miller and B. M. Harney, *Appl. Spectrosc.*, 24, 291 (1970).
(21) R. R. Holmes, G. T. Fey, and R. H. Larkin, *Spectrochim. Acta, Part A*, 29, 665 (1973).
(22) R. R. Holmes and M. Fild, *Spectrochim. Acta, Part A*, 27, 1525 (1971).
(23) R. R. Holmes and M. Fild, *Spectrochim. Acta, Part A*, 27, 1537 (1971).

Table I. Vibrational Spectrum of $[(CH_3)_3C]_2PF_3$ in the Liquid State[a]

Infrared		Raman		Polarization	Assignment[b]
cm^{-1}	I	cm^{-1}	I		
114	vw	114	vw	(p)	*t*-Bu torsion
167	vw	163	w	p	ν_8 PC_2 in-plane bend
170	vw	179	vw	(dp)	ν_{12} C_2PF in-plane bend
201	w	200	vw	(dp)	ν_{22} PCC bend
		275	m	p	ν_7 C_2PF_3 rock
293	br, sh	284	sh		ν_{23} CH_3 torsion
310	m	310	vw		ν_{11} C_2PF_2' twist
		337	w	p	ν_7 CCC bend
355	vw, br	354	vw	p	$\nu_8(C_2PF_3) + \nu_{22}(t\text{-Bu}) = 368$
394	w	394	vw	dp	ν_{21} CCC bend
427	m	430	vw	dp	ν_{10} PF_2' bend
446	w				$\nu_7 + \nu_8(C_2PF_3) = 442$
483	sh	483	w	p	$\nu_{11} + \nu_{12}(C_2PF_3) = 480$
502	s				ν_6 PF_2' bend
542	m	548	w	p	ν_5 C_2PF out-of-plane bend
583	m	584	vs	p	ν_4 PC stretch
614	m	614	w	dp	ν_9 PC asym stretch
689	vs				ν_3 PF_2' stretch
		710	vw	p	$\nu_5 + \nu_8(C_2PF_3) = 711$
734	vs				ν_2 PF_2' asym stretch
		756	w	dp	$\nu_4 + \nu_8(C_2PF_3) = 747$
807	m	807	s	p	ν_6 CC stretch
		815	w	p	$\nu_6 + \nu_{11}(C_2PF_3) = 812$
829	s	828	w	p	$\nu_{10}(C_2PF_3) + \nu_{21}(t\text{-Bu}) = 821$
867	vs	868	vw	(p)	ν_1 PF stretch
		931	w	dp	ν_{20} CH_3 rock
940	m	941	w	dp	
1015	m	1013	vw	dp	ν_{19} CH_3 rock
1023	m	1022	vw	dp	
1172	m	1184	m	p	ν_5 CH_3 rock
1215	s	1212	m	(dp)	ν_{18} CC stretch
1260	m	1260	vw	p	$\nu_1(C_2PF_3) + \nu_{21}(t\text{-Bu}) = 1261$
1284	m				$\nu_7 + \nu_{20}(t\text{-Bu}) = 1277$
1372	s	1363	vw		ν_4 CH_3 def
1400	m	1402	vw	p	ν_3 CH_3 def
		1449	m	dp	ν_{17} CH_3 def
		1464	m	dp	ν_{16} CH_3 def
1478	s				ν_{15} CH_3 def
		2710	vw	p	$\nu_{12}(t\text{-Bu}) - \nu_{12}(C_2PF_3) = 2723$
		2776	vw	p	$\nu_3 + \nu_4(t\text{-Bu}) = 2772$
		2793	vw	p	$2\nu_3(t\text{-Bu}) = 2800$
2878	s	2867	s	p	$\nu_3 + \nu_{15}(t\text{-Bu}) = 2878$
2914	s	2905	vs	p	ν_2 CH stretch
		2924	s	p	
2942	sh	2940	s	p	ν_1 CH stretch
2960	vs				ν_{14} CH stretch
		2966	s	(dp)	ν_{13} CH stretch
2998	s	2996	sh		ν_{12} CH stretch

[a] p denotes polarized; dp, depolarized; sh, shoulder; s, strong; m, medium; w, weak; v, very; ( ), uncertain. [b] Primes refer to axial atoms.

Table II. Activity of Skeletal Modes for Model Structures of $[(CH_3)_3C]_2PF_3$

Point group	Fundamentals	Raman	Ir	Raman–ir coincidences
D_{3h}	8	6 (2p)	5	3
C_{2v}	12	12 (5p)	11	11
C_s	12	12 (8p)	12	12

teristic spectrum of the *tert*-butyl group supplied by previous spectral analyses,[12,21-23] approximately 12 frequencies remain with sufficient intensity in either the infrared or Raman to serve as fundamental vibrations for the C_2PF_3 skeletal framework after subtraction of the spectrum due to the *tert*-butyl groups. Of these, five are definitely polarized. As Table II shows, structure I is definitely eliminated as a possibility with a much smaller number of bands with few coincidences expected in the infrared and Raman regions.

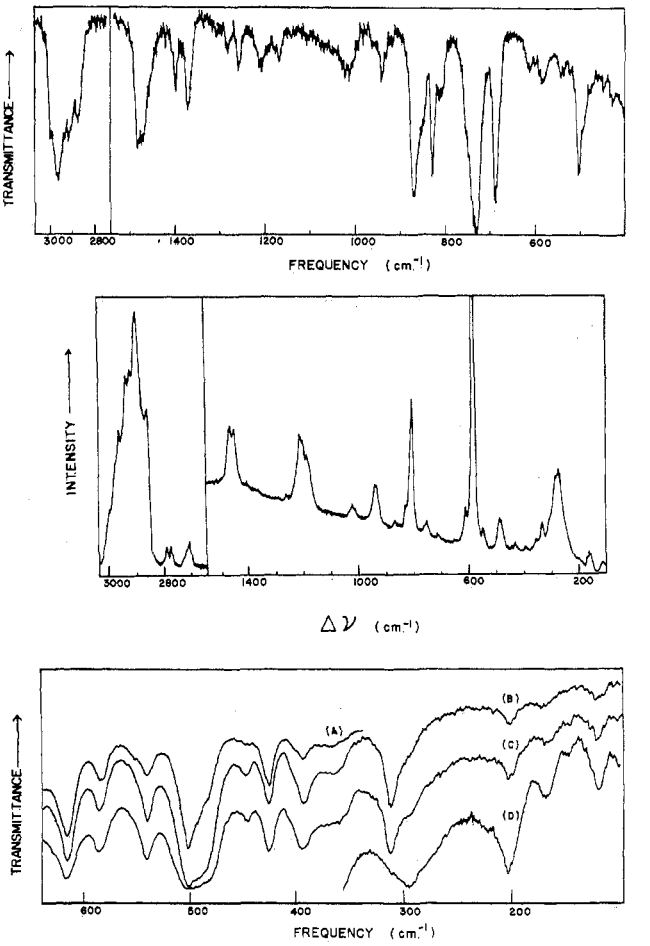

Figure 1. Vibrational spectra of $[(CH_3)_3C]_2PF_3$ in the liquid state: Top, infrared spectrum in the KBr region (liquid film); middle, argon ion Raman spectrum; bottom, far-infrared spectrum at (A) 0.1 mm, (B) 0.2 mm, (C) 0.5 mm, and (D) 0.75 mm path lengths (polyethylene windows).

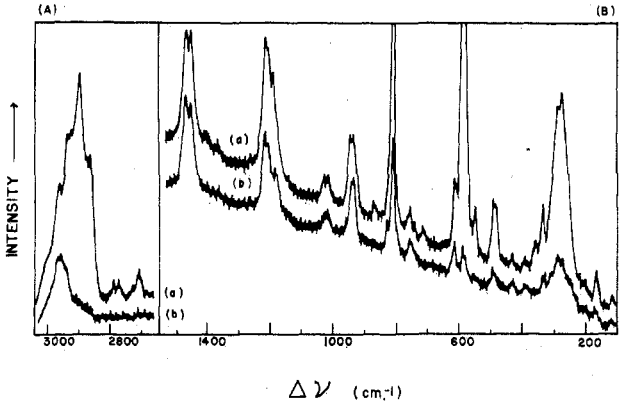

Figure 2. Polarized laser Raman spectra for $[(CH_3)_3C]_2PF_3$: (a) parallel polarization; (b) perpendicular polarization; (A) spectral band width, 6.5 cm^{-1} at 100 Δ cm^{-1}; sensitivity, 0.5 × 20,000 counts/sec; (B) spectral band width, 4.2 cm^{-1} at 100 Δ cm^{-1}; sensitivity, 0.5 × 20,000 counts/sec.

There is not much in the spectral data to differentiate between structures II and VI, although assignment to the C_{2v} point group causes some difficulty in that too many of the bending motions for the skeletal frame are polarized. Both structures have two types of fluorine atoms in the ratio of 2:1 in agreement with ^{19}F nmr observations.[14] However, there is no precedent for a square-pyramidal structure for a pentacoordinate phosphorus atom and none is suggested here. Consequently, the trigonal-bipyramidal structure II

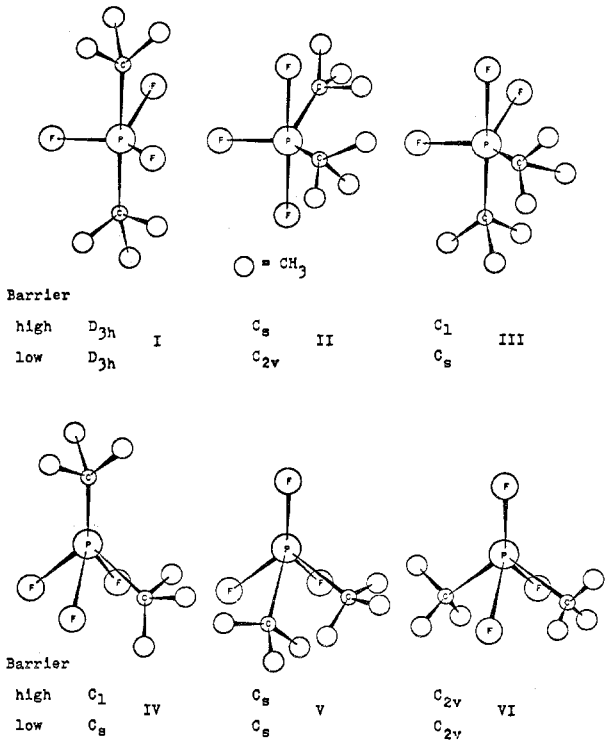

Figure 3. Structural models for $[(CH_3)_3C]_2PF_3$.

is the logical choice. It also represents the best fit to the vibrational spectrum if the high barrier case is chosen (C_s symmetry), particularly in view of the polarization data. The high barrier case is the expected one since the presence of the bulky *tert*-butyl groups located in close proximity in structure II should severely limit rotation about the P-C bonds due to their mutual steric interaction.

The detailed assignment of the *tert*-butyl groups will be outlined first, followed by consideration of the skeletal modes. If one leaves out the PC stretch (to be accounted for later under the skeletal frequencies), 19 pairs of pseudo-degenerate fundamentals should be observed for the *tert*-butyl groups under C_{3v} symmetry ($7a_1 + 12e$) active in both the infrared and Raman. In addition, four inactive a_2 vibrations are expected.

Of the 19 active fundamentals for the *tert*-butyl groups (C_{3v}), ten are internal vibrations of the methyl groups, five stretches and five bends. The CH stretches appear characteristically near 3000 cm^{-1} and the deformations are grouped near 1380 cm^{-1} and in the 1450–1480-cm^{-1} region. Most of these vibrations are readily identified in the spectra in Figure 1. The assignment of the CH stretches listed in Table I is entirely analogous to that given for $[(CH_3)_3C]_2PCl$[21] and $[(CH_3)_3C]_2PF$.[21] For the complex bands in the infrared and Raman regions near 3000 cm^{-1}, two of the lower frequency components (polarized in the Raman) are assigned to the symmetric CH stretches while three of the higher frequency components serve as CH asymmetric stretches.

Appropriately, five frequencies are assignable to the five CH_3 deformations. However, polarization data on these vibrations do not provide definitive classification in each case. Hence, assignment to species designation is made by analogy with previous assignments[21] on bis(*tert*-butyl)phosphines.

The two C-C stretches appear as before[12,21-23] near 800 and 1200 cm^{-1}. The strong infrared band at 1215 cm^{-1} with a medium intensity depolarized Raman counterpart serves as the asymmetric stretch and the strong intensity polarized Raman line at 807 cm^{-1} with a complementary infrared band at the same frequency is taken as the symmetric C-C stretch.

The methyl rocking motions (three expected, with one polarized) are assigned as the medium intensity infrared bands at 1172, 1019, and 940 cm^{-1} with corresponding Raman displacements centered at 1184 (polarized), 1018, and 936 cm^{-1}. Here, as with $[(CH_3)_3C]_2PCl$[21] and $[(CH_3)_3C]_2PF$,[21] apparent splitting of both depolarized rocking modes manifests itself. This may be an indication of the effect of the lower molecular symmetry rather than an e mode under C_{3v} symmetry assumed for the *tert*-butyl group.

Similar to that in related molecules,[12,21-23] the CCC bending modes appear weakly in the 330–400-cm^{-1} region. The most likely candidates are the polarized Raman line at 337 cm^{-1} with no infrared counterpart and the depolarized Raman line at 394 cm^{-1} with a weak infrared band appearing at the same frequency.

A C-C-P bending mode of e symmetry under C_{3v} is expected in the 150–200-cm^{-1} region. Preference is given to the Raman displacement at 200 cm^{-1}, probably depolarized, with an associated weak intensity infrared absorption at 201 cm^{-1}. In $[(CH_3)_3C]_2PF$, this frequency was assigned[21] at 202 cm^{-1}.

The only remaining fundamental to be assigned for the *tert*-butyl group is a methyl torsional mode. One might envision a broad shoulder peaking at 293 cm^{-1} in the infrared with a weak Raman feature at 284 cm^{-1}. This is the region assigned[24] to such vibrations and is given this tentative designation in Table I.

For the skeletal frame C_2PF_3 under C_s symmetry, 12 fundamentals are present, active in both the infrared and Raman ($8a' + 4a''$). Two axial and one equatorial PF stretches, all of a′ species, are to be expected. These are readily identified as the three most intense absorptions in the infrared spectrum, only one of which has any intensity in the Raman effect and that appearing very weakly. As with other pentacoordinate phosphorus fluorides,[3,7,12,13] the highest frequency stretch, 867 cm^{-1}, is assigned to the equatorial PF linkage and the lowest PF frequency, 689 cm^{-1}, to the symmetric axial stretch.

The weakness of the PF stretching modes in the Raman effect is worth noting. The same behavior occurs in $[(CH_3)_3C]_2PF$[21] and probably occurs in $(CH_3)_3CPF_4$.[12] In the latter compound, the strongest band in the Raman at 648 cm^{-1} was assigned to the equatorial PF stretch. In view of the present data, this band should be reassigned to the symmetric PC stretch. Its near degeneracy to the strong infrared band at 650 cm^{-1}, assigned to the equatorial PF stretch, led to the error in the original assignment. The much weaker band at 583 cm^{-1}, previously assigned to the PC stretch in $(CH_3)_3CPF_4$, is most likely a combination band. In addition, the band at 808 cm^{-1} in the Raman spectrum[22] of $(CH_3)_3CPF_2$, which was assigned to a PF stretch, is better assigned to the CC symmetric stretching mode. Again, the missed assignment resulted from the near degeneracy with the very intense PF stretching mode observed at 814 cm^{-1} in the infrared spectrum.

The two PC stretches are also easily assigned. These appear characteristically as the most intense, strongly polarized Raman line, here at 584 cm^{-1}, and the depolarized frequency of weak intensity at 614 cm^{-1}. Both have infrared complements of moderate intensity.

(24) J. R. Durig, S. M. Craven, and J. Bragin, *J. Chem. Phys.*, 53, 38 (1970).

Table III. Comparison of Fundamental Frequencies of X_2PF_3 Molecules (cm^{-1})

Mode description[a]	Species[b] C_{2v}	Species[b] C_s	$[(CH_3)_3C]_2PF_3$ (this work)	$(CH_3)_2PF_3$ (ref 7)	H_2PF_3 (ref 1)	Br_2PF_3[e] (ref 4)	Cl_2PF_3 (ref 28)
PF stretch	a_1	a′	ν_1 867	836	1005	913	893
PF_2' stretch			ν_3 689	540[c]	864	607	660[c,f]
PX stretch			ν_4 583	675	2482	318	407
PF_2' bend			ν_6 502	440[d]	614	420	427[f]
PX_2 in-plane bend			ν_8 167	184[c,d]	1233[c]		124[c,d]
X_2PF_2' twist	a_2	a″	ν_{11} 310	401[c]	377[c]		368
PX_2 asym stretch	b_1	a″	ν_9 614	779	2549	587	665[f]
PF_2' bend			ν_{10} 427	459[d]	472	510	488[d]
X_2PF in-plane bend			ν_{12} 170	184[c,d]	767	335	165[c,f]
PF_2' asym stretch	b_2	a′	ν_2 734	755	825	878	925
X_2PF out-of-plane bend			ν_5 542	496	1291	458	500
X_2PF_3 rock			ν_7 275[c]	471	335		338[f]

[a] Primes refer to axial atoms. [b] The molecules listed here have been assigned under C_{2v} symmetry except $[(CH_3)_3C]_2PF_3$ for which C_s symmetry forms the basis for the assignments. [c] Raman frequencies. All others listed are infrared frequencies. [d] These frequencies have been interchanged between the PF_2 axial bend and equatorial in-plane bend relative to their original assignments. In light of the discussion in ref 25 and 26, these reassignments appear more appropriate even though considerable coupling between the pairs of bending modes may exist. [e] The Raman spectrum of Br_2PF_3 was not studied. [f] These frequencies have been reassigned based on the above data on related molecules and a reinvestigation of Cl_2PF_3 (unpublished).

Seven bending modes remain to be assigned between the 160–550-cm^{-1} region, four a′ and three a″ fundamentals. Consistent with this, suggested assignments are listed in Table I and result with heavy reliance given to assignments of simpler, more symmetric phosphorus fluorides, previously examined.[3,7,13] Evidence[25,26] has supported the assignment of the lowest frequency bending modes (150–200-cm^{-1} region) to the in-plane equatorial PF motions in contrast to much higher region (425–575 cm^{-1}) normally reserved for the PF axial bends. The equatorial out-of-plane mode appears at substantially higher frequencies than the rocking and twisting fundamentals.

With these designations, only weakly appearing bands remain unassigned. These are counted as combination modes and given suggested descriptions in Table I. A low-frequency torsional mode involving the *tert*-butyl group rotating about the PC bond is given a tentative listing at 114 cm^{-1} for this very weak band appearing both in the infrared and Raman regions.

The Raman spectrum of the solid recorded at −78° remains essentially unaltered from the liquid, although some of weaker bands were not observed. This is attributed to the poorer scattering quality of the solid sample compared to the liquid and not to any significant changes in molecular structure. The weak bands tentatively assigned to torsions remain in the Raman spectrum of the solid.

Discussion

Analysis of the vibrational spectra strongly indicates a C_s point group for $[(CH_3)_3C]_2PF_3$. Consistent with nmr data,[14] the structure suggested is a trigonal bipyramid with equatorially positioned *tert*-butyl groups (Figure 3, structure II, high barrier case). Since a similar vibrational study[12] of $(CH_3)_3CPF_4$ supports a C_{2v} structure indicating a low barrier to rotation of the *tert*-butyl group about the P-C bond, it is felt that the high barrier resulting in this study is indicative of a hindering potential due primarily to the mutual steric hindrance of the two bulky *tert*-butyl groups residing in close proximity and not to the hindering potential that might be present due to repulsive interactions between the *tert*-butyl groups and the axial fluorine atoms.

An estimation of the magnitude of the barrier hindering rotation is made available from the value of the low-frequency torsional mode, tentatively identified at 114 cm^{-1}. A threefold barrier is expected to arise between the two *tert*-butyl groups as one *tert*-butyl group rotates relative to the remainder of the molecule. Approximation of reduced moments of inertia for this process and application of a cosine potential[27] result in a barrier of 12.5 kcal/mol.

It appears then that the selection rules for trigonal bipyramids of this type, for example, between C_{2v} and C_s point groups, will not break down from the higher to lower symmetry unless sizable barriers are present. In molecules like $(CH_3)_3CPF_4$, CF_3PF_4, CCl_3PF_4, CH_3PF_4, and $(CH_3)_2PF_3$, all of which have been analyzed[7,13] in terms of C_{2v} symmetry, considerably lower barriers must be present.

The assignments for the skeletal modes of $[(CH_3)_3C]_2PF_3$ are summarized in Table III and those for the *tert*-butyl group in Table IV. These are compared with similar assignments for related *tert*-butyl phosphorus fluorides[12,21,22] and other members of the X_2PF_3 series.[1,4,7,28] In agreement with the assumption of little coupling of motions between the *tert*-butyl group and the skeletal frequencies, not much variation in fundamental frequencies is seen for the modes associated with the *tert*-butyl group.

Examination of Table III reveals considerable change in frequencies for similar modes across the series, as expected, and reflects the variation in the nature of the ligands employed. However, the PF_2 axial stretching frequencies show a predictable trend. The symmetric axial stretch is more susceptible to coupling effects than the corresponding asymmetric stretch. Since each of these structures most likely has a F′-P-F′ angle mildly reduced from 180°, in accord with

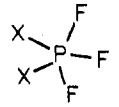

the relatively high intensity usually observed in the infrared for the symmetric PF_2 axial stretch, execution of this motion may easily involve P-F equatorial and P-X equatorial stretches. Such coupling, particularly with the symmetric PH equatorial stretch, may account for the rather high frequency, 864 cm^{-1}, assigned[1] to the PF_2 axial stretch for H_2PF_3 in Table III. Thus, without benefit of a normal coor-

(25) L. S. Bartell, *Inorg. Chem.*, 9, 1594 (1970).
(26) R. R. Holmes and J. A. Golen, *Inorg. Chem.*, 9, 1596 (1970).
(27) G. Herzberg, "Molecular Spectra and Molecular Structure. II. Infrared and Raman Spectra of Polyatomic Molecules," Van Nostrand, Princeton, N. J., 1945, pp 226–227.
(28) R. R. Holmes, *J. Chem. Phys.*, 46, 3730 (1967).

Table IV. Comparison of Fundamental Frequencies of the *tert*-Butyl Group for Fluorophosphines

No.	Mode description	Species	Frequency, cm^{-1} $[(CH_3)_3C]_2PF_3$ (this work)	$(CH_3)_3CPF_4$ (ref 12)	$[(CH_3)_3C]_2PF$ (ref 21)	$(CH_3)_3CPF_2$ (ref 22)
1	CH stretch	a_1	2942	2950	2922	2952
2	CH stretch		2914	2926	2903	2917
3	CH_3 def		1400	1410	1391	1400
4	CH_3 def		1372	1380[b]	1367	1373[b]
5	CH_3 rock		1172	1157	1176	1186
6	CC stretch		807	815[a]	805	808[c]
7	CCC bend		337[a]	355	338[a]	326
8	CH stretch	a_2				
9	CH_3 def					
10	CH_3 rock					
11	CH_3 torsion					
12	CH stretch	e	2998	3006	2967	2976
13	CH stretch		2966[a]	2988	2950	2960
14	CH stretch		2960	2977	2942[a]	
15	CH_3 def		1478	1489[b]	1474	1480[b]
16	CH_3 def		1464[a]	1472[a]	1461[a]	1471
17	CH_3 def		1449[a]	1456[a]	1450[a]	1456[a]
18	CC stretch		1215	1218	1212[a]	1204
19	CH_3 rock		1019	1028	1014	1015
20	CH_3 rock		940		946	945
21	CCC bend		394	390	393	375
22	PCC bend		201	308	202	213
23	CH_3 torsion		293	271		243

[a] Raman frequencies. Others are taken from the infrared. [b] These frequencies have been interchanged from a_1 to e or e to a_1 species compared to their original assignments. In view of the definitive polarization data on CH_3 deformations in the case of $[(CH_3)_3C]_2PF$,[21] these reassignments seem appropriate and show a consistent trend. [c] New assignment. See text.

dinate analysis, this mode is of little diagnostic value in the series under discussion.

On the other hand, the asymmetric PF_2 axial stretch gives evidence for behaving more as a characteristic frequency. A regular downward trend in frequency is apparent as the electronegativity of the attached ligand is reduced. The value[3] for this frequency in PF_5 is 945 cm^{-1}. Furthermore, in the series PF_5, CH_3PF_4, $(CH_3)_2PF_3$, and $(CH_3)_3PF_2$ a similar downward trend in axial PF stretching frequencies as methylation increases correlates[7] with increased bond lengths, both PF and PC, in line with electron-pair repulsion effects.

The same sort of reasoning may be applied here, associating a lower frequency with a longer weaker bond as anticipated from a greater electron-releasing group viewed in terms of electron-pair repulsions. Thus, $[(CH_3)_3C]_2PF_3$ should have the most distorted trigonal-bipyramidal structure with the longest, weakest PF bonds of the molecules included in Table III. As with the methylfluorophosphoranes $(CH_3)_nPF_{5-n}$, the series PF_5,[3] $(CH_3)_3CPF_4$,[12] and $[(CH_3)_3C]_2PF_3$ shows a regular downward trend in PF_2 axial stretching frequency as the number of fluorine atoms is reduced. These frequencies are 945, 846, and 734 cm^{-1}, respectively. That the trends discussed are not due to enhanced steric effects of the ligands, although they may have some influence, is demonstrated by H_2PF_3 and $(CH_3)_2PF_3$ in Table III falling in the wrong order in the electronegativity-frequency correlation.

Making the assumption, hazardous as it is, that an upfield chemical shift is associated with an enhanced electron density at the atom of interest, the general trend[15] in ^{19}F chemical shifts[8-10,14] for the series in Table III is understandable. As less electronegative ligands are used, the fluorine resonances appear at higher field indicative of greater shielding. The implication is that transmission of electron density to the fluorine atoms has paralleled the reduction in ligand electronegativity.

On further examination, other factors, however, appear to be at play. The trend[15] in ^{19}F chemical shifts[14] in the butyl series is relatively constant with increased butyl group substitution, while in the methyl series,[7,9a] a progressive downfield trend is observed with introduction of additional methyl groups, even though both series show decreased PF stretching frequencies with increased alkylation. As discussed elsewhere,[15] it is felt that the weaker bonds expected for the less fluorinated members in a series are associated with a trend toward less shielded axial fluorine atoms, as far as covalent bonding is concerned. With the presence of a group having a sufficiently high inductive effect, such as the *tert*-butyl group, enhancement of an ionic contribution may lead to a trend toward more shielded axial fluorine atoms even though the overall bond strength declines for successive members. In the PCl_nF_{5-n} series,[8,16] the downfield trend is even more pronounced than that in the methyl series.[7]

Acknowledgment. Grateful appreciation is expressed for support of this work by a grant from the National Science Foundation.

Registry No. $[(CH_3)_3C]_2PF_3$, 29120-68-1; $[(CH_3)_3C]_2PCl$, 13716-10-4.